chemosensors

MDPI

Article

Novel Electrochemical Molecularly Imprinted Polymer-Based Biosensor for Tau Protein Detection

Amira Ben Hassine [1], Noureddine Raouafi [1] and Felismina T. C. Moreira [2,3,*]

[1] Laboratory of Analytical Chemistry and Electrochemistry, Sensor and Biosensor Group, Tunis Faculty of Science, University of Tunis El Manar, Tunis El Manar 2092, Tunisia; amira.benhassine@fst.utm.tn (A.B.H.); Noureddine.raouafi@fst.utm.tn (N.R.)
[2] BioMark Sensor Research—ISEP, School of Engineering, Polytechnic Institute of Porto, 4249-015 Porto, Portugal
[3] CEB, Centre of Biological Engineering, University of Minho, 4715-000 Braga, Portugal
* Correspondence: ftm@isep.ipp.pt

Abstract: A novel electrochemical biosensor based on a molecularly imprinted polymer (MIP) was developed for the impedimetric determination of Tau protein, a biomarker of Alzheimer's disease (AD). Indeed, a recent correlation between AD symptoms and the presence of Tau proteins in their aggregated form made hyperphosphorylated Tau protein (Tangles) a promising biomarker for Alzheimer's diagnosis. The MIP was directly assembled on a screen-printed carbon electrode (C-SPE) and prepared by electropolymerization of 3-aminophenol (AMP) in the presence of the protein template (p-Tau-441) using cyclic voltammetry. The p-Tau-441 protein bound to the polymeric backbone was digested by the action of the proteolytic activity of proteinase K in urea and then washed away to create vacant sites. The performances of the corresponding imprinted and non-imprinted electrodes were evaluated by electrochemical impedance spectroscopy. The detection limit of the MIP-based sensors was 0.02 pM in PBS buffer pH 5.6. Good selectivity and good results in serum samples were obtained with the developed platform. The biosensor described in this work is a potential tool for screening Tau protein on-site and an attractive complement to clinically established methodologies methods as it is easy to fabricate, has a short response time and is inexpensive.

Keywords: electrochemical biosensor; MIPs; Tau protein; serum; Alzheimer disease

Citation: Ben Hassine A.; Raouafi, N.; Moreira, F.T.C. Novel Electrochemical Molecularly Imprinted Polymer-Based Biosensor for Tau Protein Detection. *Chemosensors* **2021**, *9*, 238. https://doi.org/10.3390/chemosensors9090238

Academic Editor: Edelmira Valero

Received: 21 July 2021
Accepted: 23 August 2021
Published: 25 August 2021

1. Introduction

AD was discovered to be a severe progressive and neurodegenerative disease leading to memory loss, personality changes, dementia, and death [1]. As this disorder becomes serious public health threat worldwide, researchers are constantly searching for new efficient tools to better understand the disease and increase the accuracy of diagnosis. to this end, biomarkers, are key to early non-invasive procedures and differential diagnosis to enable timely treatment and prevent deterioration of the patient's conditions [2].

Among the most promising and the well-described biomarkers is phosphorylated Tau protein (p-Tau) which, when used in the right clinical context, may have sufficient diagnostic accuracy and predictive power to defy both diagnostic and therapeutic challenges [3]. Indeed, this microtubule-associated protein which normally binds to and stabilizes microtubules can undergo chemical changes including proteolytic cleavage (truncation), glycation, nitration, acetylation, O-GlcNAcylation, and ubiquitination [4]. The tendency of Tau to self-associate is one of the triggers for of its dysfunction. Tau pathology is associated with the presence of insoluble filaments of Tau, but recent findings have identified soluble Tau oligomers as additional toxic species [5]. Pathological tau in AD is due to abnormal phosphorylation of Tau protein leading detachment microtubule and stacking of protein that form tangles inside neurons [6]. There are several AD biomarker-based diagnosis techniques such as mass spectrometry [7], enzyme-linked immunosorbent

assay [8], surface plasmon resonance spectrometry [9], fluorescence [10], radioimmunoassay [11], chemiluminisecence [12], and electrophoresis [13]. However, the advantages of these methods still face many limitations. Biosensors are an attractive alternative for the detection of biomolecules in samples and/or solutions in a short time with high sensitivity and specificity. This is achieved by generating a measurable signal due to the action of a transducer after capturing the desired target via a biorecognition element [14]. For this purpose, different Tau-biosensors have been developed based on the use of antibodies as a biorecognition element [15,16]. This is certainly a simple and effective way but also expensive for routine analytical measurements that require consistent reaction and redox probes and present thermal or physical instability.

Biomimetic materials are one of the most advantageous alternatives to antibodies and can be tailored using molecularly imprinted polymer technique [17]. MIP-based biosensors require the assembly of the materials on the surface of the transducer including the placement of the target to be imprinted between the selected monomeric compounds and a specific triggering of the polymerization. To achieve surface imprinting, electropolymerization as a stimulus offers several advantages such as the use of a small amount of reagent to rapidly produce f a homogeneous and thin MIP film directly on the electrode surface [18]. This technique also offers good reproducibility results and easy control of the polymer thickness [19]. So far, we report the first molecular imprinting strategy for Tau protein, whose detection limit is much lower than of that of the methods reported in the literature. Our work remains less sensitive than a single paper [16] but in return, our biosensor avoids the use of antibodies and the aid of nanomaterials for signal amplification. Thus, the method we have developed is simpler, faster, and cheaper than many previous works. It is also a specific strategy that can be applied to the study of human serum and will in the future allow distinguish between AD and normal humans in future perspectives. As the MIP is to be integrated into an electrochemical sensor, the appropriate method for polymer growth is electropolymerization. It offers numerous advantages over traditional methods such as the control of the film thickness and morphology, speed of preparation, and better adherence to the transducer surface [20]. Voltammetric electropolymerization is by far the most widely used method for electrosynthesis of polymeric films as it allows the control of the speed and sweep rate of the monomer reaction at the electrode surface. By controlling of the voltage range, it is also possible to control the polymer thickness [21]. In addition, the choice of a suitable monomer is important for the preparation of an electropolymerized MIP film. Aminophenol can be a good choice since its electropolymerized growth is self-limiting and therefore its thickness can be controlled. Due to the amino groups present in the polymeric matrix which attract the protein during the rebinding step by permeselectivity, a higher detection performance and sensitivity can be achieved [22].

Therefore, the selected monomer in this work was 3-aminophenol (AMP) which was mixed with the protein and directly electropolymerized by cyclic voltammetry (CV) on the previously activated carbon electrode surface to entrap the Tau protein in the polymeric backbone. The protein was then removed by proteolytic activity of proteinase K in urea followed by CV washes. Changes in the electrical proprieties of the working electrode and detection of the target protein were evaluated by electrochemical impedance spectroscopy (EIS) and tested both in buffer and serum systems.

EIS experiments are non-invasive tools widely used for the detection of different protein interactions and bindings and as well as for the characterization of protein's adsorption to surfaces [23–25]. The main advantages of this technique are that the protein remains intact and its conformation is not disturbed during the measurement. By using a small sample volume, EIS technique is sensitive to protein conformational change and is being extended to bioassay scaffolds for screening biomarkers and inhibitors [26].

2. Materials and Methods

2.1. Apparatus and Electrodes

Electrochemical measurements were carried out in a potentiostat/galvanostat from Metrohm Autolab, equipped with a FRA module and controlled by NOVA 2.0 software. Commercially avaiable screen-printed carbon electrodes (C-SPE) were used (Metrohm-DropSens, C-110, Coruño, Spain), which consisted of working and counter electrodes made of carbon, as well as reference electrodes and electrical contacts made of silver. The diameter of the working electrode was 4 mm. The C-SPEs were connected to a portable switch box purchased from BioTID (Vila Nova da Telha, Portugal), which allowed connection to with the potentiostat/galvanostat.

Raman measurements were performed using a Thermo Scientific DXR Raman spectrometer with confocal microscopy (Waltham, MA, USA), and a 7 mW 532 nm excitation laser. Scanning electron microscopy (SEM) analysis was performed by a high-resolution field emission gun scanning electron microscope a JEOL JSM 6301F/Oxford INCA Energy 350/Gatan Alto 2500.

2.2. Reagents and Solutions

All chemicals were of analytical grade and the water ultra-pure Milli-Q laboratory grade. Potassium hexacyanoferrate III ($K_3[Fe(CN)_6]$), potassium hexacyanoferrate II ($K_4[Fe(CN)_6]$) trihydrate, and sodium acetate anhydrous were purchased from Riedel-deHäen (Selze, Germany), Bovine serum albumin (BSA) and proteinase K from Fluka; AMP 99% from Alfa Aesar (Haverhill, MA, USA); potassium chloride (KCl) from Merck (Kenilworth, NJ, USA), hydrochloric acid (HCl) from Panreac (Barcelona, Spain); phosphate buffer saline (PBS) from Amresco (Albany, NY, USA); Urea from Fagron (Rotterdam, Netherlands); Tau protein (Tau-441) from Abcam (Cambridge, UK), Sodium Hydroxide (NaOH) from EKA (Suzhou, China); glycerine from Pronalab (Medellín, Colombia) and human serum (Cormay (Warszawa, Poland)), uric acid $\geq$99% and DL-dithiothreitol (DTT) from sigma Aldrich. 2×10^{-2} g L^{-1} Tau-444 protein was prepared in PBS buffer (1.0×10^{-3} mol L^{-1}, pH 7.4) containing 25% glycerine and 0.004% DTT and stored at -20 °C. Standards were obtained by accurate dilution of the previous solution in PBS buffer (1.0×10^{-3} mol L^{-1}, pH 5.6) or in commercial serum depending on the application. Electrochemical assays were performed with 5.0×10^{-3} mol L^{-1} $[Fe(CN)_6]^{3-}$ and 5.0×10^{-3} mol/L $[Fe(CN)_6]^{4-}$ prepared in PBS buffer pH 5.6. The selectivity study was made by a competitive assay in PBS buffer and using BSA (1.0×10^{-2} g L^{-1}) and uric acid (1.0×10^{-3} g L^{-1}).

2.3. Design of the Biosensor

In the first step, the C-SPEs were cleaned and activated with a KCl solution (0.1 mol L^{-1}) using the chronoamperometry procedure (+1.7 V for 400 s) and gently washed off with Milli-Q water (Figure 1a). The imprinting of the protein on the working surface was achieved by CV-based polymerization (between -0.2 and 1.2 V at a scan rate of 50 mVs^{-1}, for 5 cycles) after covering the three electrodes of the C-SPE with 50 µL of a solution containing AMP 1.0×10^{-3} mol L^{-1} and Tau 2.0×10^{-3} g L^{-1} in PBS pH 5.6 (Figure 1b). A wash step was then performed with Milli-Q water, followed by incubation with proteinase K (500 gm L^{-1} in PBS pH 7.4) in 0.5% for 2.5 h at room temperature (Figure 1c). After protein removal, another washing step with Milli-Q water followed by CV-based electrochemical stabilization in PBS buffer pH 5.6 (between -0.2 and +1.2 V, scan rate 50 mVs^{-1}, for 10 cycles). this was followed by rebinding of the target protein in the formed cavities in the film was performed by a 30 min incubation with increasing concentrations of the standard solutions of serum samples. After a final wash, the three-electrode system was fully covered with the iron redox probe solution for the electrical measures.

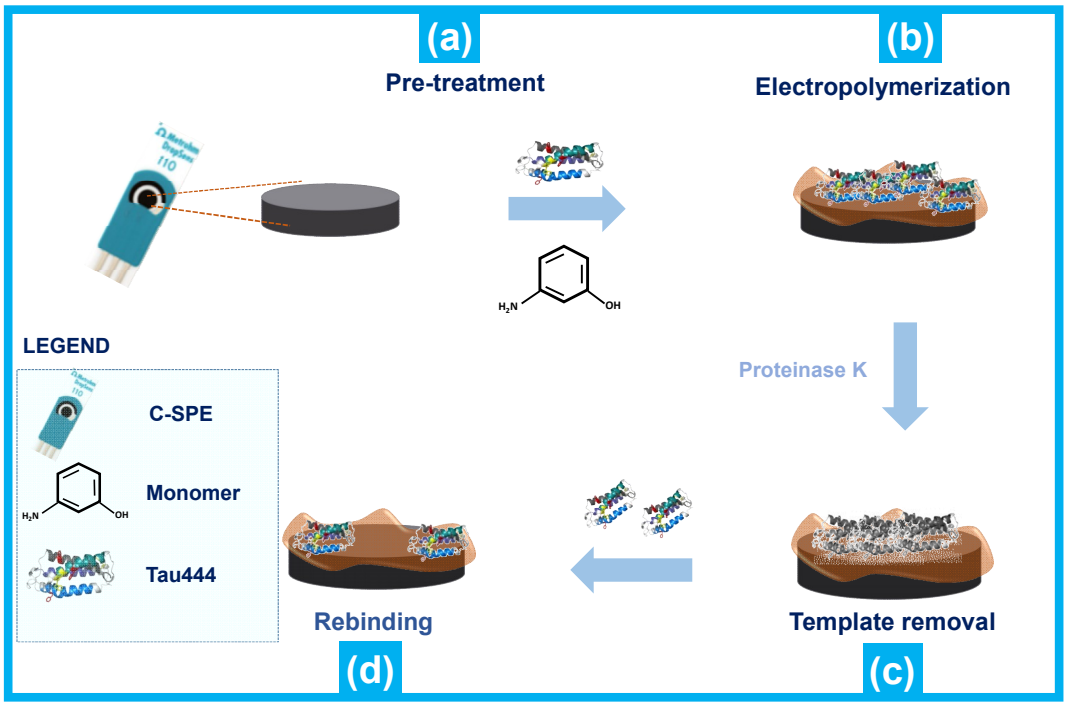

Figure 1. Schematic diagram of the electrochemically assisted MIP strategy and the sequence of reactions involved in the impedimetric transduction at C-SPEs for the determination of Tau protein.

All steps performed in the preparation of the Tau platform with molecularly imprinted polymers (MIPs) are schematically presented in Figure 1. The same strategy was adopted for the non-imprinted polymers (NIPs) the difference is that the target protein is missing in the polymer backbone. To monitor the success of the different steps, methods such as CV, square wave voltammetry (SWV), and EIS were carried out and presented throughout the process.

2.4. Qualitative Characterization of the Films

All qualitative investigations of the different steps describing the biorecognition film were directly performed on the C-SPE without any prior treatment. Imprinted films with Tau-444 protein and after the removal step as well as non-imprinted films were analyzed by Raman spectroscopy. The average signal-to-noise ratio (peak height/RMS noise) was automatically put as 5 min as maximum measurement time, with a laser power of 7 mW on the sample, and a slit aperture of 50. SEM analysis was done at high vacuum and 1 × 105 magnification at 15 kV. Images were taken of the dried C-SPE, the MIP, and the NIP material at several locations of each sample.

2.5. Electrochemical Assays

The redox probes in all SWV, CV, and EIS measurements consisted of 5.0 mmol L^{-1} $[Fe(CN)_6]^{3-}$ and 5.0 mmol/L $[Fe(CN)_6]^{4-}$ prepared in PBS buffer at pH 5.6. In the SWV and CV assays, the potential range was from −0.2 to +0.5 V. In the EIS, an open circuit potential was settled through a sinusoidal potential perturbation of 0.01 V amplitude and 50 as frequency values that were logarithmically distributed over a range of frequencies between 0.01 Hz and 100 kHz. Calibrations were performed by EIS measurements for Tau-441 protein in the range of 2.18 pM to 2.18 nM. At each concentration from the selected range, 5 µL of the target was incubated in PBS buffer for 30 min at room temperature on the embossed sensor surface.

The selectivity of the developed platform was tested by the competitive method and using BSA and uric acid in PBS buffer at pH 5.6 as interfering elements.

The response of the MIP sensor was tested for solutions containing only p-Tau 441 protein 218 pM or p-Tau 441 + interfering species, since it can be assumed that Tau and interfering species compete for the same binding sites. For this purpose, the signal of the Tau protein alone (considering its signal of 100%) was compared with the mixture of Tau protein and interfering species.

Real sample analysis was carried out by spiking Tau protein in commercial serum (1:1000, serum/PBS buffer) using the same protocol.

3. Results and Discussion

As shown in Figure 2, the developed platform was based on the MIP strategy and was developed by electropolymerisation of the monomer AMP by CV using the Tau-441 protein as the template molecule. The overall process involved three main steps: (1) the imprinting step by forming a poly(AMP)film containing the target protein on the electrode surface; (2) the removal of the protein from the film by proteinase K in urea; and (3) the rebinding of the protein. The different phases led to changes in the electron transfer properties of the receptor surface and were therefore followed by EIS, SWV, and CV tests involving $[Fe(CN)_6]^{3-}/[Fe(CN)_6]^{4-}$ redox probe.

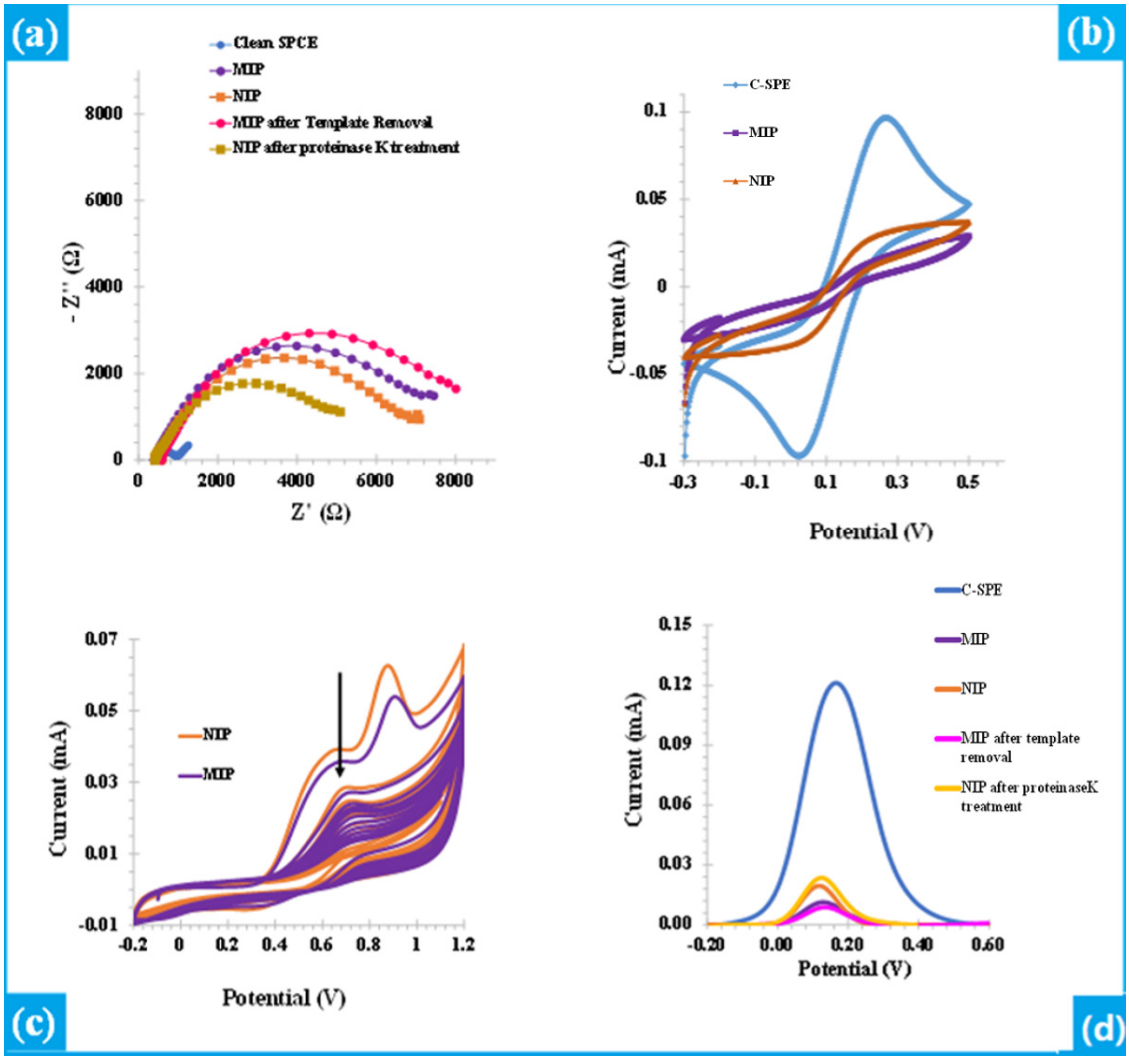

Figure 2. Follow up of the different steps for MIP and NIP films (**a**) EIS data (**b**) CV data (**c**) electrochemical polymerization of MIP and NIP film at C-SPEs (10 cycles) and (**d**) SWV data. The standard iron redox probes were 5.0 mM $[Fe(CN)_6]^{3-}$ and 5.0 mM $[Fe(CN)_6]^{4-}$ solution in PBS buffer pH 5.6.

3.1. Choice of the Platform Elements

MIPs-based platforms offer several advantages over immunosensors and other techniques. However, several parameters have to be carefully selected in order to make good exploitation of this methodology. Indeed, the selection of the adequate elements for the target biorecognition is very important and depends on several criteria such as the polymerization degree, the potential range for the electropolymerization, and the functional groups present in the selected polymer [27,28]. The family of polyaminophenols is advantageous for these effects with a high degree of permselectivity and simple control of the polymer density that can self-limit its growth. In addition, the stability of the target protein is favoured by its interaction with the amine and hydroxyl groups during the rebinding step [29]. Experiments on electropolymerisation were carried out with both 2-aminophenol and 3-aminophenol. However, with 2-aminophenol it was not possible to obtain a stable measurement after electrochemical measurements. Therefore, 3-aminophenol was chosen as the monomer for the rest of the study (Figure S1). Furthermore, a polymerisation with 10 CV cycles was tested, which resulted in a lower resistance at the electrode surface after the polymerisation step (Figure S1). This result can be explained by the detachment and loss of the polymer at a higher number of cycles during polymerisation. The loss of the formed polymer led to the creation of a very low number of protein capture sites, resulting in a low sensitivity of the developed platform (Figure S2). Another important step in the design of our platform is the removal of the template. Indeed, there are several ways to remove the protein entrapped in the embossed film by chemical or enzymatic methods. In this case, the target was removed in the form of peptide fragments by the proteolytic action of proteinase K in urea. The removal was followed by washing with PBS and electrochemical stabilisation (successive CVs).

3.2. Electropolymerization and Imprinting Step

Before starting the imprinting step, the C-SPEs were pre-treated to ensure the electrochemical oxidation of all materials or impurities present on the working electrode. This included a chronoamperometric activation in a solution of 0.1 M KCl, for 400 s at +1.7 V. After this step, the redox probe mediator signal on CV showed a current increase compared to bare unmodified C-SPEs and a lower potential difference between oxidation and reduction peaks of the probe. This current increase was coupled to a huge decrease in Rct (EIS) as shown in Figure S3.

The polymeric film was generated over the pre-treated C-SPEs by conducting an electropolymerization of AMP mixed with Tau protein by applying 5 consecutive CV cycles (Figure 2c). In the first cycle of the electropolymerization, for both MIP and NIP, only two current peaks in the oxidation potentials are observed at 0.65 and 0.9 V with a higher signal intensity obtained with the NIP. In the next cycles, the anodic currents were continuously decreasing. However, the peak about 0.9 V is more prominent and is representative of the oxidation of the amino group of the *meta*-aminophenol (please see Figure 2c) [30–33]. The current peak indicated the occurrence of electropolymerization, with a lower current measured in MIP layers compared to NIP. The small current difference was due to the presence of the protein on the MIP layer. However, the absence of a cathodic peak proves the irreversibility of the reaction, while the decrease in anodic currents confirms the production and growth of a blocking surface from the desired polymer.

The data from CV (Figure 2b) and SWV (Figure 2d) obtained with both the MIP and NIP coatings the C-SPEs displayed a huge decrease in the redox peaks of the iron probe after the imprinting step (83% and 66% of decrease in the MIP and NIP CV peaks, respectively). These conditions demonstrate the presence of a higher blocked surface confirming the presence of a non-conductive and electro-inactive polymeric film on the working electrode surface. The difference in the redox probe currents drop between MIP and NIP could be attributed to the presence of the protein in MIP which could interfere in the electropolymerization process. EIS measurements were also conducted to follow the electrical changes at the surface electrodes (Figure 2a).

In general, the EIS data fitted into the simplified Randles equivalent circuit describing the different changes occurring at the electrode-solution interface. This circuit included one resistor element. Semicircles were observed at a high-frequency range indicating (solution resistance, Rs) in series with one parallel circuit consisting of a resistor (charge transfer resistance, Rct) and a double layer capacitance (Cdl) [34]. In the Randles circuit, the Nyquist plot consists of a semicircle observed in the high-frequency range and a linear behaviour in the low-frequency range. The semicircles indicate a process controlled by charge transfer and intersect the real axis (Z)at two points. The first one revealed the solution resistance value (Rs) and the second one indicates the total resistance (Rs + Rct). Thus, the electron-transfer kinetics of the redox-probe at the electrode-solution interface was controlled by the charge-transfer electrode (Rct) which corresponds to the diameter of the semi-circle [35]. The enlargement of the semicircles observed after the electropolymerization shows that the non-conducting polymeric film strongly increases in the resistance of the electrode. The activated C-SPE revealed a very small semicircle corresponding to a low Rct value compared to the semicircle after the imprinting modifications. However, the modifications of the charge-transfer resistance were different in MIP compared to the NIP which yielded to higher Rct value (8160 and 7470 Ω, respectively). This difference could be attributed to the presence of the protein. The presence of the Tau-441 protein in the solution could impact the electrical properties of the surface where the polymer is growing. This directly affected the polymer growth yielding different results between NIP and MIP.

Furthermore, the Tau protein has an isoelectric point comprised between 9.5 and 6.5 due to the exonic encoding cassettes and post-transitional modifications [36]. Hence working at a pH 5.6 could allow a positive charge to grow up over the surface, in the case of MIP interacting with the Tau protein. This induced the attraction of an increased number of negatively charged iron redox probes on the surface [37].

3.3. Protein Removal Step

The impedimetric results (Figure 2a) obtained with the MIP platform after the template removal step might be different than expected as protein removal generally decreases the resistance of the studied surface. However, the 10% increase of Rct in our case could be attributed to the protein protonation compared to the redox probe. If Tau protein could be positively protonated, the concentration of the iron redox probe at the surface could increase by ionic interaction. This would reduce the Rct value despite the existence of a higher amount of a non-conductive compound at the surface. These predictions were lately verified by incubating different concentrations of Tau on a bare electrode, resulting in bare electrode, resulting in a decrease in resistance Hence, the Rct increase in the MIP platform after the proteinase K activity can be caused by protein loss.

The SWV data (Figure 2d) resulted after template removal step showed a 33% decrease that the redox peaks of the iron probe decreased in the MIPs-modified electrode confirming the protein loss. The NIP platforms adopted an opposite behaviour after this step.

3.4. Follow-Up of the Surface Modification

3.4.1. Raman Spectroscopy

Raman spectra were recorded with a 532 nm laser at different stages of the biosensor assembly for both MIP and NIP materials (Figure 3).

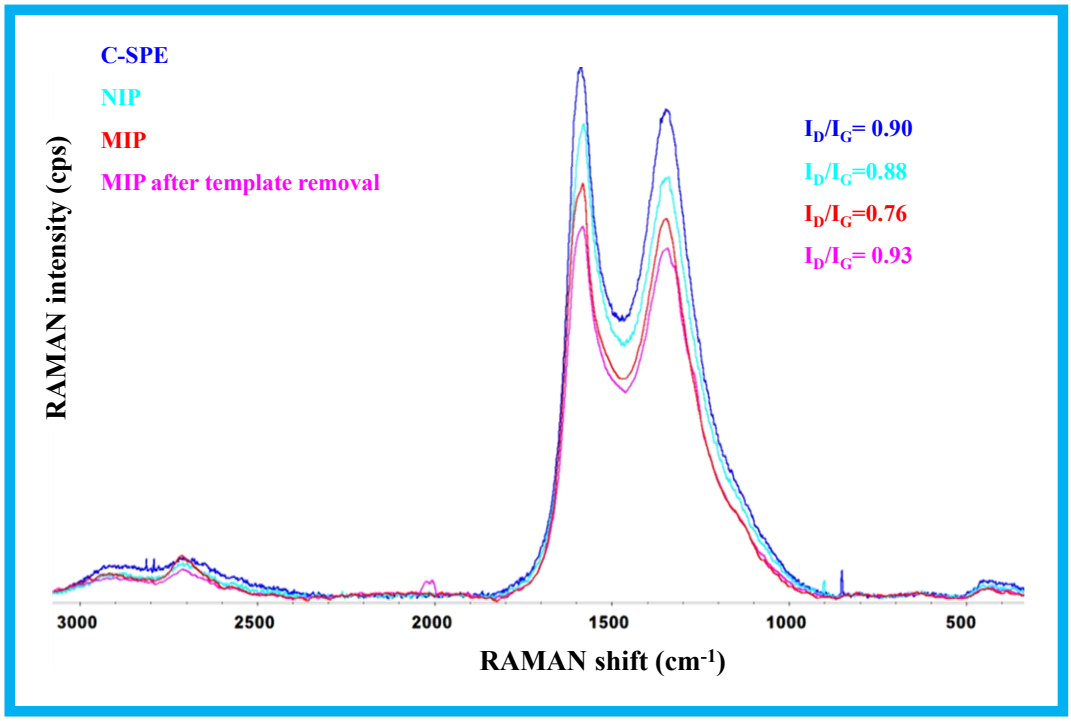

Figure 3. Raman spectra of C-SPE, MIP before and after template removal and NIP.

The Raman spectra provided valuable information about the chemical changes on the electrode surface and allowed tracking of each step. In general, two prominent peaks (G and D bands) were clearly visible in all Raman spectra, indicating the presence of a carbon-based matrix. The G peak appeared at ~1580 cm^{-1} corresponding to the C-C stretching of the first-order scattering of the sp2 carbon hybridization, while the D peak was at ~1340 cm^{-1}, corresponding to the carbon defects originating from the sp3 carbon hybridization [38]. The I_D/I_G ratio usually indicates the extent of disorder in a material, hence changes in this intensity ratio may reflect the disorder introduced with the carbon material after each chemical change [39].

Before any modification, the C-SPE presented a ratio of 0.90 which considerably decreased after MIP film imprinting to 0.76 and only 0.88 for NIP film. However, the ratio increased from 0.76 to 0.93 for the MIP film after template removal.

The difference in the ratios can be attributed to the different matrix formation at the surface of NIP and MIP. The presence of Tau in the polymer backbone also affected the ratio, as the MIP (0.76) had a lower ratio compared to the bare C-SPE (0.90) and the platform NIP (0.88). The increase in the ratio for the MIP after removal (0.93) of the template indicates a higher presence of defects in the structure after the proteolytic action of proteinase K. This could be due to the presence of voids in the polymer matrix, which introduce defects in the structure of carbons by breaking the sp2 structure. Moreover, both MIP and NIP showed similar behaviour in terms of broader peak shape, which is consistent with the fact that the chemical composition of these films was similar.

3.4.2. Scanning Electron Microscopy

SEM analysis (Figure S4) was performed for C-SPE, MIP, and NIP materials. By SEM analysis it is not possible to confirm the imprinting effect because the morphology of MIP and NIP materials was similar. However, the chemical modification of the C-SPE with MIP and NIP materials was easily detected. The thicker and denser layer observed after the imprinting process is due to the presence of the polymer on the surface.

3.4.3. Analytical Features of the Sensor

The performance of developed biosensor was carried out by applying the same strategy for both MIP and NIP and finally by incubation with Tau standard solution with increasing concentration. The calibrations curves conducted in EIS are shown in Figure 4b with a concentration range between 2.18 pM and 2.18 nM. Figure 4a the EIS spectra after the addition of different Tau concentrations for the MIP device.

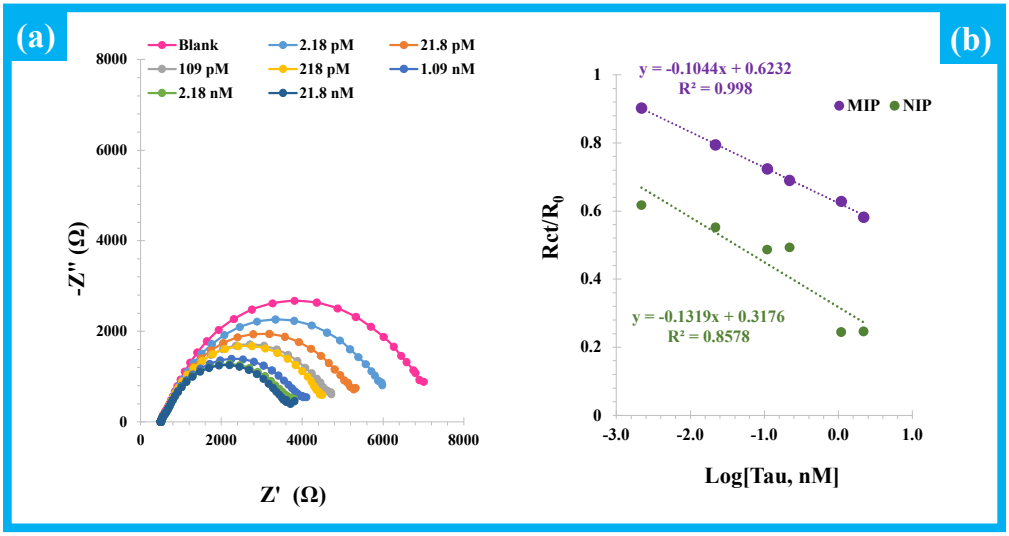

Figure 4. (**a**) EIS measurements of MIPs and (**b**) the corresponding calibration curves of MIP (purple) and NIP (green) in 5.0 mM $[Fe(CN)_6]^{3-}$ and 5.0 mM $[Fe(CN)_6]^{4-}$, in PBS buffer pH 5.6, with different concentrations of Tau protein.

The calibration curve of the MIP host polymer displayed a linear response over a wide range of Tau concentrations (between 2.18 pM and 2.18 nM), linear slope −0.104/log[Tau 441, nM] and detection limit (LOD) of 0.024 pM considering three times the standard deviation of the blank response. However, the NIP-based platform showed a random behavior in the presence of an increasing concentration of the target protein confirming that only the binding sites of the MIP-based device could recognize and accumulate the Tau protein. The precision of the MIP-based platforms (three different measurements were done using three different electrodes), at different levels of concentration, is presented in Figure S5

3.4.4. Selectivity

The competitive method was used to evaluate the selectivity of the developed biosensor regarding non-target compounds. All parameters were maintained as in the calibration assays and EIS measurements were also conducted in the same conditions. BSA and uric acid were selected as potential interferences to the target protein. Despite the high ratio of 1:1000 between the target protein and the interferences, a signal variation of only 4.5% and 4.6%was observed for BSA and uric acid, respectively (Figure 5). This confirms the selectivity of the recognition sites created in the polymer film toward the target protein.

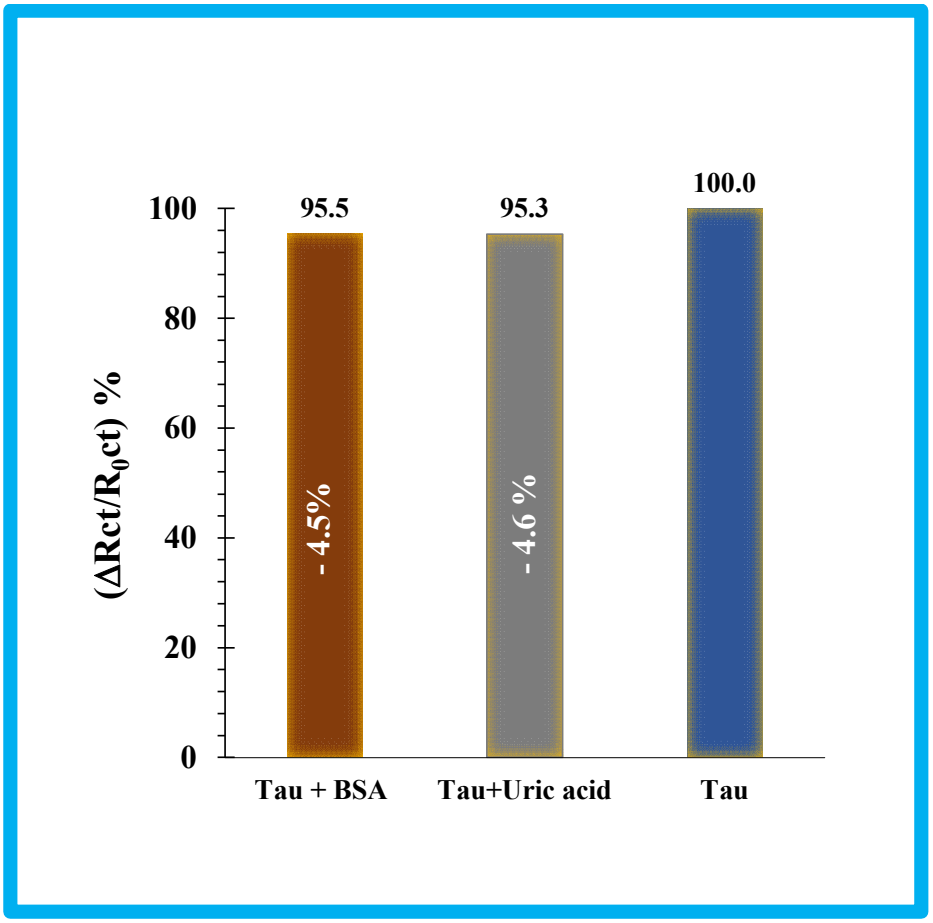

Figure 5. Selectivity test of the sensor by competitive method; signal for mixture of Tau and BSA, mixture of Tau and Uric acid, and only Tau protein.

3.4.5. Application to Real Samples

Our biosensor's accuracy for routine analysis was evaluated using the standard addition method. Different concentrations were spiked human serum diluted 1000 times and EIS measurements were performed (Figure 6). Using this matrix, a LOD of 0.067 pM and a linear slope of −0.155[Tau 441, nM] (32% higher than in PBS buffer) was obtained, which was slightly higher than the LOD obtained in the PBS buffer. This slight difference is likely due to the presence of other molecules and other Tau proteins that may interact with the rebinding sites of the film or with the target protein, thus affecting the sensing results. The recovery factors were tested after spiking the protein in diluted serum samples. The spiked value was 2.18 nM and the recovered value was 2.02 nM. This was equivalent to a recovery value of 92%.

As shown in Table 1, our platform is the first MIP-based strategy for the detection of Tau and the obtained detection limit is lower than almost all previous work with the advantage of not using nanomaterials or any costly products such as antibodies, as is the case for immunosensors.

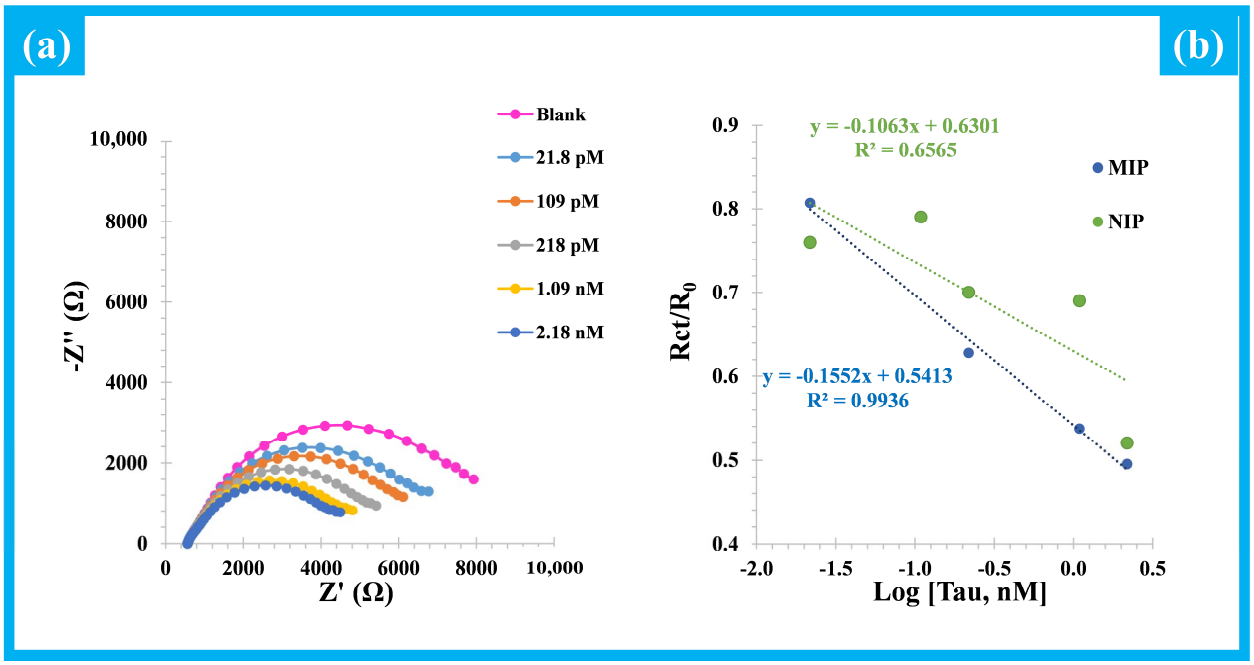

Figure 6. EIS measurements of (**a**) MIPs based biosensor and the corresponding calibration curves (**b**) in 5.0 mM $[Fe(CN)_6]^{3-}$ and 5.0 mM $[Fe(CN)_6]^{4-}$ by spiking Tau protein in serum.

Table 1. Biosensors to detect Tau protein.

Method	Technique	Target	Biorecognition Element	LOD	Samples	Year	Ref.
Electrochemical	EIS	Tau-441	Antibody	0.03 pM (LOQ)	serum	2016	[15]
	DPV	Tau-381	Aptamer	0.7 pM	serum	2019	[40]
	DPV	Tau-441	Antibody	0.46 fM	Serum	2020	[16]
	EIS	Tau-441	Antibody	-	-	2018	[41]
	DPV	T-Tau	Antibody	-	Serum	2017	[42]
Optical	Fluorescence	Tau	Antibody	0.14 pM	-	2017	[43]
	SPR	Tau	Sandwich assay	2 nM	-	2017	[44]
	SERS	Tau-381	Antibody	25 fM	-	2013	[45]
	SPR	Tau-381	Aptamer	10 fM	plasma	2016	[46]

4. Conclusions

The main goal of this work was to develop the first molecularly imprinted polymer -based device for a promising AD biomarker, the Tau protein. In contrast to the optical and electrochemical biosensors described in the literature for the detection of the Tau protein (Table 1), our strategy avoided the use of expensive materials, such as antibodies, and complicated immobilization materials such as aptamers. The plastic antibodies were electrochemically synthesized and simply assembled and showed good overall performance. The non-imprinted films showed random results, making this biosensor particularly suitable for the detection of Tau protein.

Our strategy was to achieve simple and inexpensive assembly while maintaining good precision, selectivity, and low detection limit. Together with the advantages of disposability, portability, and simplicity of the device, a promising future for the point-of-care field can be expected after further experiments have ensured its application in real samples.

Supplementary Materials: The following are available online at https://www.mdpi.com/article/10.3390/chemosensors9090238/s1, Figure S1: Electrochemical EIS spectra after the electrpolymerization with 3-aminophenol using 5 cycles and 10 cycles of CV; Figure S2: EIS measurements of (A) MIPs based biosensor and the corresponding calibration curves (B) in 5.0 mM $[Fe(CN)_6]^{3-}$ and 5.0 mM

$[Fe(CN)^6]^{4-}$ in PBS buffer in the case of the electropolymerization step with 10 CV cycles; Figure S3: Electrochemical EIS spectra (A) and CV voltammograms (B) for C-SPE surface before and after KCl pretreatment (evaluated in 5.0 mmol/L $[Fe(CN)_6]^{3-}$ and 5.0 mmol/L $[Fe(CN)_6]^{4-}$, in PBS pH 5.6) [6]; Figure S4: SEM images of the C-SPE, MIP and NIP materials; Figure S5: Reproducibility study of the MIP.

Author Contributions: Conceptualization, F.T.C.M.; methodology, A.B.H.; validation, A.B.H. formal analysis, F.T.C.M. and A.B.H.; investigation, A.B.H.; resources, F.T.C.M.; writing—original draft preparation, A.B.H.; writing—review and editing, F.T.C.M. and N.R.; supervision, F.T.C.M. and N.R.; project administration F.T.C.M.; funding acquisition, F.T.C.M. All authors have read and agreed to the published version of the manuscript.

Funding: 0624_2IQBIONEURO_6_E, 2QBioneuro, Impulso de una red de I + i en química biológica para diagnóstico y tratamiento de enfermedades neurológicas EP-INTERREG V A España Portugal (POCTEP).

Institutional Review Board Statement: Not applicable.

Informed Consent Statement: Not applicable.

Data Availability Statement: Not applicable.

Acknowledgments: A.B.H. acknowledges the University of Tunis El Manar for the mobility grant "Bourse d'alternance". 0624_2IQBIONEURO_6_E, Impulso de una red de I + i en química biológica para diagnóstico y tratamiento de enfermedades neurológicas EP-INTERREG V A España Portugal (POCTEP).

Conflicts of Interest: The authors declare no conflict of interest.

References

1. Hampel, H.; Prvulovic, D.; Teipel, S.; Jessen, F.; Luckhaus, C.; Frölich, L.; Riepe, M.W.; Dodel, R.; Leyhe, T.; Lars, B.; et al. The future of Alzheimer's disease: The next 10 years. *Prog. Neurobiol.* **2011**, *95*, 718–728. [CrossRef]
2. Foster, J.; Sohrabi, H.; Verdile, G.; Martins, R. Research criteria for the diagnosis of Alzheimer's disease: Genetic risk factors, blood biomarkers and olfactory dysfunction. *Int. Psychogeriatr.* **2008**, *20*, 853–855. [CrossRef]
3. Hampel, H.; Blennow, K. CSF tau and β-amyloid as biomarkers for mild cognitive impairment. *Dialogues Clin. Neurosci.* **2004**, *6*, 379.
4. Panza, F.; Solfrizzi, V.; Seripa, D.; Imbimbo, B.P.; Lozupone, M.; Santamato, A.; Tortelli, R.; Galizia, I.; Prete, C.; Daniele, A.; et al. Tau-based therapeutics for Alzheimer's disease: Active and passive immunotherapy. *Immunotherapy* **2016**, *8*, 1119–1134. [CrossRef] [PubMed]
5. Elbaum-Garfinkle, S.; Rhoades, E. Identification of an aggregation-prone structure of tau. *J. Am. Chem. Soc.* **2012**, *134*, 16607–16613. [CrossRef]
6. Grundke-Iqbal, I.; Iqbal, K.; Tung, Y.-C.; Quinlan, M.; Wisniewski, H.M.; Binder, L.I. Abnormal phosphorylation of the microtubule-associated protein tau (tau) in Alzheimer cytoskeletal pathology. *Proc. Natl. Acad. Sci. USA* **1986**, *83*, 4913–4917. [CrossRef]
7. Barthélemy, N.R.; Bateman, R.J.; Hirtz, C.; Marin, P.; Becher, F.; Sato, C.; Gabelle, A.; Lehmann, S. Cerebrospinal fluid phospho-tau T217 outperforms T181 as a biomarker for the differential diagnosis of Alzheimer's disease and PET amyloid-positive patient identification. *Alzheimer's Res. Ther.* **2020**, *12*, 26. [CrossRef] [PubMed]
8. Hu, Y.Y.; He, S.S.; Wang, X.; Duan, Q.H.; Grundke-Iqbal, I.; Iqbal, K.; Wang, J. Levels of nonphosphorylated and phosphorylated tau in cerebrospinal fluid of Alzheimer's disease patients: An ultrasensitive bienzyme-substrate-recycle enzyme-linked immunosorbent assay. *Am. J. Pathol.* **2002**, *160*, 1269–1278. [CrossRef]
9. Vestergaard, M.D.; Kerman, K.; Kim, D.-K.; Hiep, H.M.; Tamiya, E. Detection of Alzheimer's tau protein using localised surface plasmon resonance-based immunochip. *Talanta* **2008**, *74*, 1038–1042. [CrossRef] [PubMed]
10. Liu, C.; Lu, D.; You, X.; Shi, G.; Deng, J.; Zhou, T. Carbon dots sensitized lanthanide infinite coordination polymer nanoparticles: Towards ratiometric fluorescent sensing of cerebrospinal Aβ monomer as a biomarker for Alzheimer's disease. *Anal. Chim. Acta* **2020**, *1105*, 147–154. [CrossRef]
11. Smith, C.D.; Wekstein, D.R.; Markesbery, W.R.; Frye, C.A. 3α, 5α-THP: A potential plasma neurosteroid biomarker in Alzheimer's disease and perhaps non-Alzheimer's dementia. *Psychopharmacology* **2006**, *186*, 481–485. [CrossRef] [PubMed]
12. Agnello, L.; Piccoli, T.; Vidali, M.; Cuffaro, L.; Lo Sasso, B.; Iacolino, G.; Giglio, V.R.; Lupo, F.; Alongi, P.; Bivona, G.; et al. Diagnostic accuracy of cerebrospinal fluid biomarkers measured by chemiluminescent enzyme immunoassay for Alzheimer disease diagnosis. *Scand. J. Clin. Lab. Investig.* **2020**, *80*, 313–317. [CrossRef] [PubMed]
13. Verpillot, R.; Otto, M.; Klafki, H.; Taverna, M. Simultaneous analysis by capillary electrophoresis of five amyloid peptides as potential biomarkers of Alzheimer's disease. *J. Chromatogr. A* **2008**, *1214*, 157–164. [CrossRef]
14. Metkar, S.K.; Girigoswami, K. Diagnostic biosensors in medicine—A review. *Biocatal. Agric. Biotechnol.* **2019**, *17*, 271–283. [CrossRef]

15. Wang, S.X.; Acha, D.; Shah, A.J.; Hills, F.; Roitt, I.; Demosthenous, A.; Bayford, R.H. Detection of the tau protein in human serum by a sensitive four-electrode electrochemical biosensor. *Biosens. Bioelectron.* **2017**, *92*, 482–488. [CrossRef]
16. Li, X.; Jiang, M.; Cheng, J.; Ye, M.; Zhang, W.; Jaffrezic-Renault, N.; Guo, Z. Signal multi-amplified electrochemical biosensor for voltammetric determination of tau-441 protein in biological samples using carbon nanomaterials and gold nanoparticles to hint dementia. *Microchim. Acta* **2020**, *187*, 302. [CrossRef]
17. Frasco, M.F.; Truta, L.A.; Sales, M.G.F.; Moreira, F.T.C. Imprinting technology in electrochemical biomimetic sensors. *Sensors* **2017**, *17*, 523. [CrossRef]
18. Elshafey, R.; Radi, A.-E. Electrochemical impedance sensor for herbicide alachlor based on imprinted polymer receptor. *J. Electroanal. Chem.* **2018**, *813*, 171–177. [CrossRef]
19. Guo, Z.; Florea, A.; Cristea, C.; Bessueille, F.; Vocanson, F.; Goutaland, F.; Zhang, A.; Sandculescu, R.; Lagarde, F.; Jaffrezic-Renault, N. 1,3,5-Trinitrotoluene detection by a molecularly imprinted polymer sensor based on electropolymerization of a microporous-metal-organic framework. *Sens. Actuators B Chem.* **2015**, *207*, 960–966. [CrossRef]
20. Gomes, R.S.; Moreira, F.T.C.; Fernandes, R.; Sales, M.G.F. Sensing CA 15–3 in point-of-care by electropolymerizing O-phenylenediamine (oPDA) on Au-screen printed electrodes. *PLoS ONE* **2018**, *13*, e0196656. [CrossRef]
21. Crapnell, R.D.; Hudson, A.; Foster, C.W.; Eersels, K.; Grinsven, B.V.; Cleij, T.J.; Banks, C.E.; Peeters, M. Recent advances in electrosynthesized molecularly imprinted polymer sensing platforms for bioanalyte detection. *Sensors* **2019**, *19*, 1204. [CrossRef]
22. Moreira, F.T.C.; Sharma, S.; Dutra, R.A.F.; Noronha, J.P.C.; Cass, A.E.G.; Sales, M.G.F. Protein-responsive polymers for point-of-care detection of cardiac biomarker. *Sens. Actuators B Chem.* **2014**, *196*, 123–132. [CrossRef]
23. Ostatná, V.; Černocká, H.; Paleček, E. Simple protein structure-sensitive chronopotentiometric analysis with dithiothreitol-modified Hg electrodes. *Bioelectrochemistry* **2012**, *87*, 84–88. [CrossRef] [PubMed]
24. Bartošík, M.; Ostatná, V.; Paleček, E. Electrochemistry of riboflavin-binding protein and its interaction with riboflavin. *Bioelectrochemistry* **2009**, *76*, 70–75. [CrossRef] [PubMed]
25. Bogomolova, A.; Komarova, E.; Reber, K.; Gerasimov, T.; Yavuz, O.; Bhatt, S.; Aldissi, M. Challenges of electrochemical impedance spectroscopy in protein biosensing. *Anal. Chem.* **2009**, *81*, 3944–3949. [CrossRef] [PubMed]
26. Bard, A.J.; Faulkner, L.R. Fundamentals and applications. *Electrochem. Methods* **2001**, *2*, 580–632.
27. Chen, L.; Wang, X.; Lu, W.; Wu, X.; Li, J. Molecular imprinting: Perspectives and applications. *Chem. Soc. Rev.* **2016**, *45*, 2137–2211. [CrossRef] [PubMed]
28. Yarman, A.; Jetzschmann, K.J.; Neumann, B.; Zhang, X.; Wollenberger, U.; Cordin, A.; Haupt, K.; Scheller, F.W. Enzymes as Tools in MIP-Sensors. *Chemosensors* **2017**, *5*, 11. [CrossRef]
29. Erdossy, J.; Horvath, V.; Yarman, A.; Scheller, F.W.; Gyurcsanyi, R.E. Electrosynthesized molecularly imprinted polymers for protein recognition. *TrAC Trends Anal. Chem.* **2016**, *79*, 179–190. [CrossRef]
30. Mu, S. Electrochemical copolymerization of aniline and o-aminophenol. *Synth. Met.* **2004**, *143*, 259–268. [CrossRef]
31. Dinc, C.O.; Yalcinkaya, S.; Altuntas, H.; Colak, N. Synthesis and characterization of poly(m-aminophenol)-succinat. *Des. Monomers Polym.* **2014**, *17*, 629–636. [CrossRef]
32. Tucceri, R.A.P.; Scian, A. Electrosynthesis and Spectroscopic Characterization of Poly(*o*-Aminophenol) Film Electrodes. *ISRN Polym. Sci.* **2012**, *2012*, 26. [CrossRef]
33. Salavagione, H.J.; Arias, J.; Garces, P.; Morallon, E.; Barbero, C.; Vazquez, J.L. Spectroelectrochemical study of the oxidation of aminophenols on platinum electrode in acid medium. *J. Electroanal. Chem.* **2004**, *565*, 375–383. [CrossRef]
34. Daniels, J.S.; Pourmand, N. Label-free impedance biosensors: Opportunities and challenges. *Electroanal. Int. J. Devoted Fundam. Pract. Asp. Electroanal.* **2007**, *19*, 1239–1257. [CrossRef] [PubMed]
35. Suni, I.I. Impedance methods for electrochemical sensors using nanomaterials. *TrAC Trends Anal. Chem.* **2008**, *27*, 604–611. [CrossRef]
36. Sergeant, N.; Bretteville, A.; Hamdane, M.; Caillet-Boudin, M.-L.; Grognet, P.; Bombois, S.; Blum, D.; Delacourte, A.; Pasquier, F.; Vanmechelen, E.; et al. Biochemistry of Tau in Alzheimer's disease and related neurological disorders. *Expert Rev. Proteom.* **2008**, *5*, 207–224. [CrossRef]
37. Khan, M.A.R.; Moreira, F.T.C.; Riu, J.; Sales, M.G.F. Plastic antibody for the electrochemical detection of bacterial surface proteins. *Sens. Actuators B Chem.* **2016**, *233*, 697–704. [CrossRef]
38. Kudin, K.N.; Ozbas, B.; Schniepp, H.C.; Prud'Homme, R.K.; Aksay, I.A.; Car, R. Raman spectra of graphite oxide and functionalized graphene sheets. *Nano Lett.* **2008**, *8*, 36–41. [CrossRef] [PubMed]
39. Suprun, E.V.; Radko, S.P.; Khmeleva, S.A.; Mitkevich, V.A.; Archakov, A.I.; Makarov, A.A.; Shumyantseva, V.V. Electrochemical oxidation of amyloid-beta peptide isoforms on carbon screen printed electrodes. *Electrochem. Commun.* **2017**, *75*, 33–37. [CrossRef]
40. Tao, D.; Shui, B.; Gu, Y.; Cheng, J.; Zhang, W.; Jaffrezic-Renault, N.; Song, S.; Guo, Z. Development of a label-free electrochemical aptasensor for the detection of Tau381 and its preliminary application in AD and non-AD patients' sera. *Biosensors* **2019**, *9*, 84. [CrossRef]
41. Carlin, N.; Martic-Milne, S. Anti-tau antibodies based electrochemical sensor for detection of tau protein biomarkers. *J. Electrochem. Soc.* **2018**, *165*, G3018. [CrossRef]
42. Dai, Y.; Molazemhosseini, A.; Liu, C.C. A single-use, in vitro biosensor for the detection of T-tau protein, a biomarker of neuro-degenerative disorders, in PBS and human serum using differential pulse voltammetry (DPV). *Biosensors* **2017**, *7*, 10. [CrossRef] [PubMed]

43. Huang, A.; Zhang, L.; Li, W.; Ma, Z.; Shuo, S.; Yao, T. Controlled fluorescence quenching by antibody-conjugated graphene oxide to measure tau protein. *R. Soc. Open Sci.* **2018**, *5*, 171808. [CrossRef] [PubMed]
44. Lisi, S.; Scarano, S.; Fedeli, S.; Pascale, E.; Cicchi, S.; Ravelet, C.; Peyrin, E.; Minunni, M. Toward sensitive immuno-based detection of tau protein by surface plasmon resonance coupled to carbon nanostructures as signal amplifiers. *Biosens. Bioelectron.* **2017**, *93*, 289–292. [CrossRef]
45. Zengin, A.; Tamer, U.; Caykara, T. A SERS-based sandwich assay for ultrasensitive and selective detection of Alzheimer's tau protein. *Biomacromolecules* **2013**, *14*, 3001–3009. [CrossRef] [PubMed]
46. Kim, S.; Wark, A.W.; Lee, H.J. Femtomolar detection of tau proteins in undiluted plasma using surface plasmon resonance. *Anal. Chem.* **2016**, *88*, 7793–7799. [CrossRef] [PubMed]